Temperature dependence of London penetration depth anisotropy in superconductors with anisotropic order parameters

V. G. Kogan [*]

Ames Laboratory, DOE, Ames, Iowa 50011, USA

R. Prozorov [†]

Ames Laboratory, DOE, Ames, Iowa 50011, USA
and Department of Physics and Astronomy, Iowa State University, Ames, Iowa 50011, USA

We study the effects of anisotropic order parameters on the temperature dependence of London penetration depth anisotropy $\gamma_\lambda(T)$. After MgB$_2$, this dependence is commonly attributed to distinct gaps on multiband Fermi surfaces in superconductors. We have found, however, that the anisotropy parameter may depend on temperature also in one-band materials with anisotropic order parameters $\Delta(T, \boldsymbol{k}_F)$; a few such examples are given. We have also found that for different order parameters, the temperature dependence of $\Delta(T)/\Delta(0)$ can be represented with good accuracy by the interpolation suggested by Einzel [J. Low Temp. Phys **131**, 1 (2003)], which simplifies considerably the evaluation of $\gamma_\lambda(T)$. Of particular interest are mixed order parameters of two symmetries for which $\gamma_\lambda(T)$ may go through a maximum for a certain relative weight of two phases. Also, for this case we find that the ratio $\Delta_{\max}(0)/T_c$ may exceed substantially the weak-coupling limit of 1.76. It, however, does not imply strong coupling; rather, it is due to significantly anisotropic angular variation of Δ.

I. INTRODUCTION

The London penetration depth λ is one of the major characteristics of superconductors. Most materials studied nowadays are anisotropic with complicated Fermi surfaces and nontrivial order parameters $\Delta(\boldsymbol{k})$ ($\boldsymbol{k}$ is the Fermi momentum). As a result, λ is also anisotropic; in uniaxial materials of interest here the λ anisotropy is characterized by the anisotropy parameter $\gamma_\lambda = \lambda_c/\lambda_a$ (a and c stand for principal crystal directions). For a long time γ_λ has been considered a temperature-independent constant. With the discovery of MgB$_2$ [1] it was found that $\gamma_\lambda(T)$ increases on warming [2] due to two different gaps on two groups of Fermi surface sheets [3,4]. Since then, if a T dependence of γ_λ is observed, it is commonly attributed to a multigap type of superconductivity. We show below that, in fact, γ_λ depends on T also in the one-band case if the order parameter Δ is anisotropic even on isotropic Fermi surfaces.

We focus on the clean limit for two major reasons. Commonly, after discovery of a new superconductor, an effort is made to obtain single crystals as clean as possible since they are better for studying the underlying physics. In addition, in general, the scattering suppresses the anisotropy of λ, the quantity of interest in this work.

Although our formal results are written in the form applicable to any Fermi surface, we consider only Fermi spheres to separate effects of the order parameter symmetry on the anisotropy of λ from the effects of anisotropic Fermi surfaces. Another reason is experimental: There are materials currently

studied with a nearly isotropic upper critical field but with unusual nonmonotonic $\gamma_\lambda(T)$ [5].

To our knowledge, up to now, theoretical work on the temperature dependence of γ_λ has been focused on evaluation of γ_λ at $T = 0$ and T_c [6]. Assuming monotonic behavior of $\gamma_\lambda(T)$, the knowledge of γ_λ at the end points suffices for a qualitative description of this dependence. This assumption, however, is challenged by recent data on nonmonotonic $\gamma_\lambda(T)$ [5].

To evaluate the temperature dependence of the penetration depth and its anisotropy, one first has to calculate the equilibrium order parameter $\Delta(T)$, a nontrivial and time-consuming task because one has to solve the self-consistency equation of the theory (the gap equation). Instead, one can employ a version of the interpolation scheme of Einzel [7–9], which provides an accurate representation of the BCS gap dependence $\Delta(T)$ for various order parameter symmetries. Moreover, we show that, in fact, the reduced $\Delta(T)/\Delta(0)$ as a function of reduced temperature $t = T/T_c$ has a nearly universal form for all order parameters we tested. This simplifies remarkably the task of evaluating $\Delta(T)$. We note, however, that all temperature-dependent results shown after Fig. 1 were obtained using numerically exact solutions of the self-consistency equation (8).

II. APPROACH

Weak-coupling superconductors are described by a system of quasiclassical Eilenberger equations [10]. For a clean material in the absence of field, the Eilenberger functions f and g satisfy [10]

$$0 = \Delta g - \omega f, \tag{1}$$
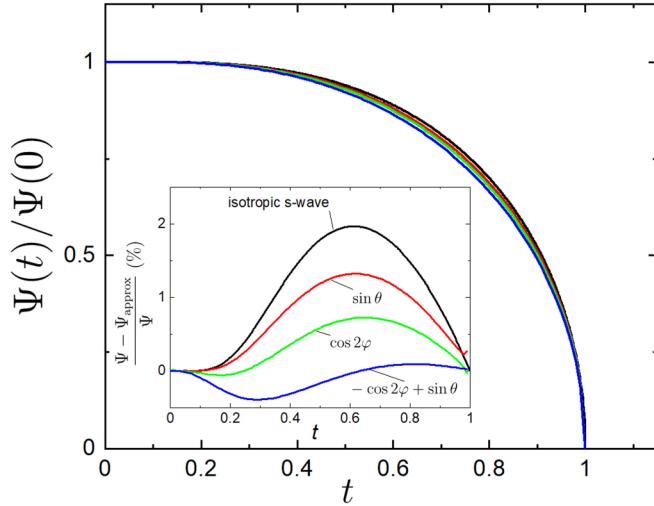$$1 = g^2 + f^2. \tag{2}$$

*kogan@ameslab.gov
†prozorov@ameslab.gov

FIG. 1. The order parameter $\Psi(T)/\Psi(0)$ according to Eq. (14). The black curve is the isotropic s wave, $\Omega = 1$. The red curve is for the clean sample with polar nodes, $\Omega = \sqrt{3/2}\sin\theta$, with θ being the polar angle on the Fermi sphere. The green curve is for the d wave with $\Omega = \sqrt{2}\cos 2\varphi$, and the blue one is for $\Omega \propto (\sin\theta - \cos 2\varphi)$. The inset shows the difference between exact $\Psi(t)$ obtained by numerically solving the self-consistency Eq. (8) and interpolations (14) for the indicated order parameters.

Here, Δ is the superconducting order parameter, which might depend on the position at the Fermi surface, and $\omega = \pi T(2n+1)$ are Matsubara frequencies; hereafter $\hbar = 1$ and $k_B = 1$. This system yields

$$f = \Delta/\sqrt{\Delta^2 + \omega^2}, \quad g = \omega/\sqrt{\Delta^2 + \omega^2}. \quad (3)$$

All equilibrium properties of uniform superconductors can be expressed in terms of f and g.

Within the separable model [11], the coupling responsible for superconductivity is assumed to have the form $V(\boldsymbol{k}, \boldsymbol{k}') = V_0 \Omega(\boldsymbol{k})\Omega(\boldsymbol{k}')$, which leads to

$$\Delta(T, \boldsymbol{k}) = \Psi(T)\Omega(\boldsymbol{k}). \quad (4)$$

The function $\Omega(\boldsymbol{k})$ is normalized [12]:

$$\langle \Omega^2 \rangle = 1, \quad (5)$$

where $\langle \cdots \rangle$ stands for averaging over the Fermi surface. This normalization is convenient, enough to mention the condensation energy at $T = 0$ [13]:

$$F(0) = \frac{N(0)}{2}\langle \Delta^2(0) \rangle = \frac{N(0)}{2}\Psi^2(0), \quad (6)$$

where $N(0)$ is the density of states per spin.

The self-consistency equation which provides the temperature-dependent order parameter $\Psi(T)$ reads [4]

$$\frac{\Psi}{2\pi T}\ln\frac{T_c}{T} = \sum_{\omega > 0}\left(\frac{\Psi}{\omega} - \langle \Omega f \rangle\right), \quad (7)$$

with T_c being the critical temperature. The dimensionless form of this equation is

$$-\ln t = \sum_{n=0}^{\infty}\left(\frac{1}{n+1/2} - \left\langle\frac{\Omega^2}{\sqrt{(n+1/2)^2 + \Omega^2\delta^2/t^2}}\right\rangle\right), \quad (8)$$

where n is the Matsubara integer, $t = T/T_c$, and $\delta = \Psi/2\pi T_c$. Clearly, the solution $\delta(t)$ depends on the anisotropy of the order parameter given by Ω.

In particular, one obtains [8,13] (see also the Appendix)

$$\frac{\Psi(0)}{T_c} = \frac{\pi}{e^\gamma}e^{-\langle\Omega^2\ln|\Omega|\rangle}. \quad (9)$$

If $T \to T_c$, Eq. (8) yields

$$\Psi^2(T) = \frac{8\pi^2 T_c^2}{7\zeta(3)\langle\Omega^4\rangle}\left(1 - \frac{T}{T_c}\right). \quad (10)$$

Einzel constructed a remarkably good approximation to the T dependence of the order parameter [7–9]:

$$\frac{\Psi(t)}{\Psi(0)} = \tanh\left(\frac{T_c}{\Psi(0)}\sqrt{\frac{8\pi^2(1-t)}{7\zeta(3)\langle\Omega^4\rangle t}}\right). \quad (11)$$

A more accurate interpolation can be constructed by including terms of the order $(1-t)^2$ [9].

For $t \to 1$ we readily obtain Eq. (10). If $t \to 0$, $\Psi(t) \to \Psi(0)$ and deviates from $\Psi(0)$ exponentially slowly due to the tanh function.

At low temperatures, one uses $\tanh x \approx 1 - 2e^{-2x}$ to obtain, from Eq. (11),

$$\frac{\Psi(t)}{\Psi(0)} = 1 - 2\exp\left(-\frac{T_c}{\Psi(0)}\sqrt{\frac{8\pi^2}{7\zeta(3)\langle\Omega^4\rangle t}}\right). \quad (12)$$

This differs from the BCS result,

$$\frac{\Delta(t)}{\Delta(0)} = 1 - \sqrt{\frac{2\pi T}{\Delta(0)}}e^{-\Delta(0)/T}. \quad (13)$$

Although Eq. (11) does not reproduce correctly an exponentially small deviation of Ψ from $\Psi(0)$ at low temperatures, it generates there a flat behavior so that in numerical evaluation this difference may not matter.

Using $\Psi(0)/T_c$ from Eq. (9), we rewrite (11) in the form

$$\frac{\Psi(t)}{\Psi(0)} = \tanh\left(e^\gamma\sqrt{\frac{8(1-t)}{7\zeta(3)t}}\frac{e^{\langle\Omega^2\ln|\Omega|\rangle}}{\sqrt{\langle\Omega^4\rangle}}\right). \quad (14)$$

Hence, we can evaluate the ratio $\Psi(t)/\Psi(0) = \Delta(t)/\Delta(0)$ for any particular Ω.

The order parameter $\Delta(t)/\Delta(0)$ for point polar nodes, normalized to its value at $T = 0$, is shown in Fig. 1 by the red curve. The isotropic case is shown in black for comparison, the green curve is for the d wave, and the blue curve is for a mixed order parameter. One can say that in the chosen reduced units all these curves overlap within a few percent accuracy. One can also say that one cannot deduce the type of order parameter from the measured ratio $\Delta(t)/\Delta(0)$.

III. $\gamma_\lambda(T)$

To consider the system response to a weak field, one turns to the full set of Eilenberger equations:

$$\boldsymbol{v}\boldsymbol{\Pi}f = 2\Delta g - 2\omega f, \quad (15)$$

$$-\boldsymbol{v}\boldsymbol{\Pi}^* f^+ = 2\Delta^* g - 2\omega f^+, \quad (16)$$

$$g^2 = 1 - f f^+. \quad (17)$$

Here, v is the Fermi velocity, $\Pi = \nabla + 2\pi i A/\phi_0$, A is the vector potential, and ϕ_0 is the flux quantum; f and g now depend on coordinates.

Weak supercurrents and fields leave the order parameter modulus unchanged but cause the condensate to acquire an overall phase $\chi(r)$. We therefore look for perturbed solutions of the Eilenberger system in the form

$$\Delta e^{i\chi}, \quad (f_0 + f_1)e^{i\chi}, \quad (f_0 + f_1^+)e^{-i\chi}, \quad g_0 + g_1, \quad (18)$$

where f_0 and g_0 refer to the uniform zero-field state discussed above and the subscript 1 marks corrections due to small perturbations $v\Pi$. In the London limit, the only coordinate dependence is that of the phase χ; that is, f_1 and g_1 are r independent too.

The Eilenberger equations (15)–(17) provide the corrections among which we need only g_1:

$$g_1 = \frac{if_0^2 vP}{2(\Delta_0 f_0 + \omega g_0)} = \frac{if_0^2}{2\beta_0} vP. \quad (19)$$

Here, the supermomentum $P = \nabla\theta + 2\pi A/\phi_0 \equiv 2\pi a/\phi_0$, with the "gauge-invariant vector potential" a, and $\beta_0^2 = \omega^2 + \Delta_0^2$. Substituting this in the general expression for the current density

$$j = -4\pi|e|N(0)T \ \text{Im} \sum_{\omega>0} \langle vg \rangle \quad (20)$$

and comparing the result with the London current $4\pi j_i/c = -(\lambda^2)_{ik}^{-1} a_k$, we obtain [4]

$$(\lambda^2)_{ik}^{-1} = \frac{16\pi^2 e^2 N(0)T}{c^2} \sum_\omega \left\langle \frac{\Delta^2 v_i v_k}{\beta^3} \right\rangle. \quad (21)$$

Since only unperturbed values of Δ and β enter this expression, the subscript 0 is omitted.

Hence, we have for the T dependence of the anisotropy $\gamma_\lambda^2(T) = \lambda_{cc}^2/\lambda_{aa}^2$ of uniaxial materials

$$\gamma_\lambda^2(t) = \frac{\langle \Omega^2 v_a^2 \sum_\omega [\omega^2 + \Psi^2(t)\Omega^2]^{-3/2} \rangle}{\langle \Omega^2 v_c^2 \sum_\omega [\omega^2 + \Psi^2(t)\Omega^2]^{-3/2} \rangle}. \quad (22)$$

In particular, we have

$$\gamma_\lambda^2(0) = \frac{\langle v_a^2 \rangle}{\langle v_c^2 \rangle}, \quad \gamma_\lambda^2(T_c) = \frac{\langle \Omega^2 v_a^2 \rangle}{\langle \Omega^2 v_c^2 \rangle}. \quad (23)$$

The result for $\gamma_\lambda^2(T_c)$ is originally due to Gor'kov and Melik-Barkhudarov [14].

Thus, the general scheme for evaluation of $\lambda(T)$ consists of two major steps: first, evaluate the order parameter $\Delta_0(T)$ in the uniform zero-field state, then use Eq. (21) with a proper averaging over the Fermi surface. The sum over Matsubara frequencies is fast convergent and is done numerically, except in limiting situations for which analytic evaluation is possible.

We now consider a few cases of different order parameters on a one-band Fermi sphere and show that, depending on the order parameter, the anisotropy $\gamma_\lambda(T)$ might increase or decrease monotonically on warming or even be a nonmonotonic function of T.
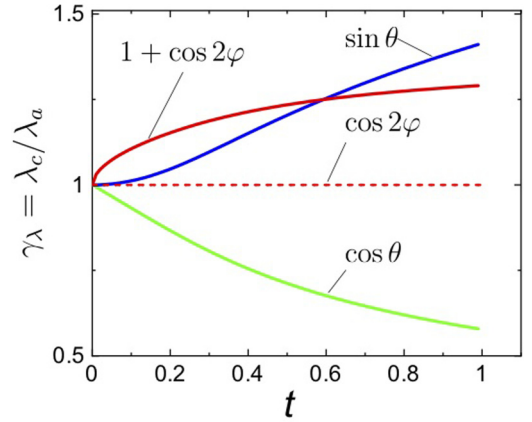

FIG. 2. Anisotropy parameters γ_λ vs the reduced temperature t for the order parameter with polar point nodes $\Omega = \sqrt{3/2}\sin\theta$ (blue line), the equatorial line node $\sqrt{3}\cos\theta$ (green line), and the d wave $\sqrt{2}\cos 2\varphi$ (dashed red line). The curve $1 + \cos 2\varphi$ for mixed s and d order parameters increases with t, despite the fact that s and d separately have t-independent $\gamma_\lambda = 1$.

A. d wave

For the d wave $\Omega = \sqrt{2}\cos 2\varphi$. We find $\langle\Omega^2 \ln|\Omega|\rangle = (1 - \ln 2)/2$ and $\Psi(0)/T_c = \sqrt{2}\pi e^{-0.5-\gamma} \approx 1.513$, whereas $\Delta_{\max}(0)/T_c = (\Psi(0)/T_c)\sqrt{2} = 2.14$. The ratio that enters interpolation (14) is

$$\rho = \frac{e^{\langle\Omega^2 \ln\Omega^2\rangle/2}}{\langle\Omega^4\rangle} \approx 0.78. \quad (24)$$

To evaluate $\gamma_\lambda(t)$, we need the t dependence of the order parameter given in Eq. (14). The numerical evaluation then gives $\gamma_\lambda(t) = 1$, in agreement with earlier calculations of end points $\gamma_\lambda(0) = \gamma_\lambda(T_c) = 1$ [6].

B. Polar nodes on the Fermi sphere

We model this case by setting $\Omega = \sqrt{3/2}\sin\theta$. We readily find $\gamma_\lambda^2(T_c) = 2$. Further, we obtain

$$\frac{1}{2}\langle\Omega^2 \ln\Omega^2\rangle = \frac{\ln 216 - 5}{6} \approx 0.0626 \quad (25)$$

and the parameter $\rho \approx 0.89$. The anisotropy parameter evaluated numerically as described above is shown by the blue curve in Fig. 2, which shows that $\gamma_\lambda(t)$ increases. If $\Omega \propto \cos\theta$, the same numerical procedure yields the decreasing $\gamma_\lambda(t)$. Interestingly, a pure d-wave order parameter $\Omega = \sqrt{2}\cos 2\varphi$ as well as pure s-wave order parameter $\Omega = 1$ produce a temperature-independent $\gamma_\lambda(t) = 1$, whereas their mixture, e.g., $1 + \cos 2\varphi$, gives an increasing $\gamma_\lambda(t)$.

To check the accuracy of Einzel's approximation for $\Psi(T)$ we did all the calculations based on Eilenberger's theory *per se*, and we found no noticeable differences.

C. Equatorial line node

This type of line node was suggested as possible in some Fe-based materials [15,16] and observed in angle-resolved photoemission spectroscopy (ARPES) experiments [17]. For
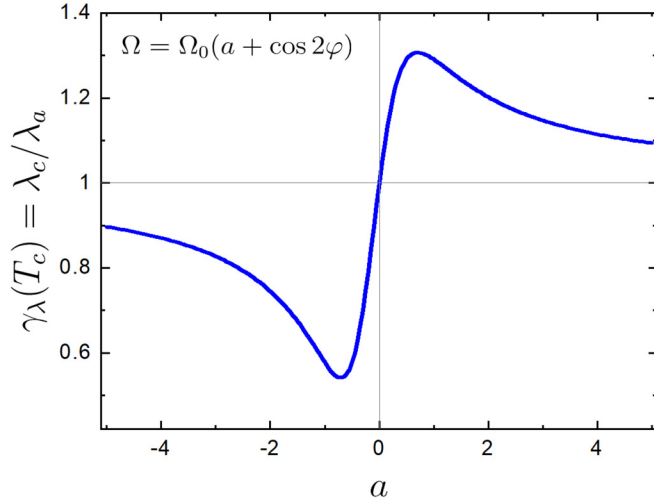
FIG. 3. $\gamma_\lambda(T_c)$ vs a for the order parameter $\Omega = \Omega_0(a + \cos 2\varphi)$.

the order parameter $\Omega = \sqrt{3}\cos\theta$ we evaluate

$$\frac{1}{2}\langle\Omega^2\ln\Omega^2\rangle = \frac{\ln 27 - 2}{6} \approx 0.216, \quad (26)$$

and the parameter $\rho \approx 0.69$. The corresponding $\gamma_\lambda(t)$ is shown by the green curve in Fig. 2. Thus, on the basis of this and the previous example we conclude that, depending on the order parameter, γ_λ may increase or decrease on warming even in one-band systems.

D. $\Omega = \Omega_0(a + \cos 2\varphi)$

$\Omega = \Omega_0(a + \cos 2\varphi)$ corresponds to a mixed s- and d-wave order parameter, a possibility considered for cuprates (see, e.g., [18,19]).

The anisotropy parameter $\gamma_\lambda(T_c)$ vs a is shown in Fig. 3. Since on a Fermi sphere $\gamma_\lambda^2(0) = 1$, we see that for $a > 0$ the anisotropy $\gamma_\lambda(T)$ grows on warming, whereas for negative a it decreases. Surprising at first sight, this means that for mixed order parameters $\gamma_\lambda(T)$ depends on relative phases of the order parameters in the mixture; in this case for $a < 0$ the phase difference is π.

The top curve in Fig. 4 shows the parameter $\langle\Omega^4\rangle$, which affects the specific heat jump [9,18,19],

$$\frac{\Delta C}{C_n(T_c)} = \frac{12}{7\zeta(3)\langle\Omega^4\rangle} \approx \frac{1.426}{\langle\Omega^4\rangle}. \quad (27)$$

The bottom curve is the parameter $\langle\Omega^2\ln|\Omega|\rangle$, which enters the ratio $\Psi(0)/T_c$, Eq. (9). Since this parameter is small at all a, one has

$$\Psi(0)/T_c \approx 1.76(1 - \langle\Omega^2\ln|\Omega|\rangle). \quad (28)$$

In fact, $\langle\Omega^2\ln|\Omega|\rangle < 1$ in all examples we have considered.

E. $\Omega = \Omega_0(a + \sin\theta)$

$\Omega = \Omega_0(a + \sin\theta)$ corresponds to a mixture of the s wave and the phase with polar nodes. It is instructive to study this case because positive a's make the condensate a nodeless anisotropic s wave, whereas $a < 0$ turns the polar nodes into line nodes along certain altitude circles. We start with the
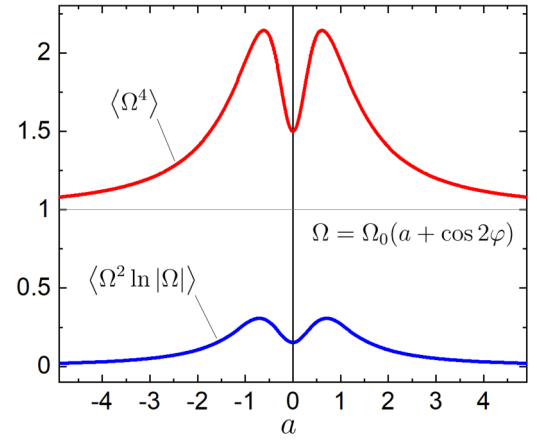

FIG. 4. The top curve is $\langle\Omega^4\rangle$ vs a, and the bottom curve is $\langle\Omega^2\ln|\Omega|\rangle$ for the order parameter $\Omega = \Omega_0(a + \cos 2\varphi)$.

normalization $\langle\Omega^2\rangle = 1$, which yields

$$\Omega_0^2 = \frac{2}{4/3 + \pi a + 2a^2}. \quad (29)$$

Next, we calculate

$$\langle\Omega^4\rangle = \frac{4}{(4/3 + \pi a + 2a^2)^2}\langle(a + \sin\theta)^4\rangle$$

$$= 2\frac{16/15 + 8a^2 + 2a^4 + 3\pi a/2 + 2\pi a^2}{(4/3 + \pi a + 2a^2)^2}. \quad (30)$$

This function is plotted in Fig. 5. The maximum of this curve at $a_m \approx -0.888$ means that the order parameter near T_c in Eq. (10) along with the specific heat jump is suppressed at a_m by about a factor of 5 relative to the pure s wave.

It is instructive also to plot the ratio $\Delta(0)/T_c$, which is traditionally considered a distinguishing parameter for weak and strong couplings. If the order parameter is anisotropic, $\Delta(0)_{max}/T_c$ is usually measured. Using Eq. (9), we obtain

$$\frac{\Delta(0; a, \theta)}{T_c} = \frac{\Psi(0)\Omega(a, \theta)}{T_c} = \frac{\pi\Omega}{e^\gamma}e^{-\langle\Omega^2\ln|\Omega|\rangle}. \quad (31)$$
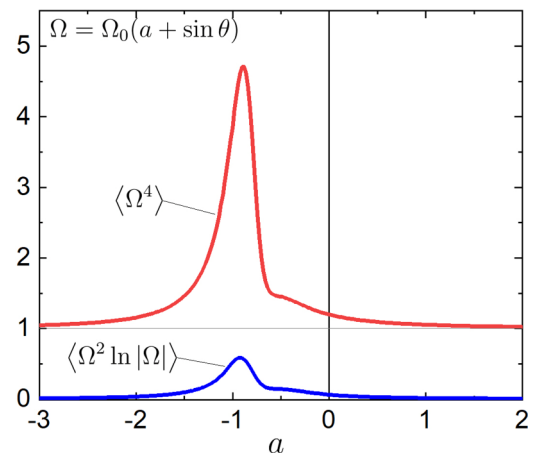

FIG. 5. $\langle\Omega^4\rangle$ and $\Omega^2\ln|\Omega|$ vs a for the order parameter $\Omega = \Omega_0(a + \sin\theta)$.
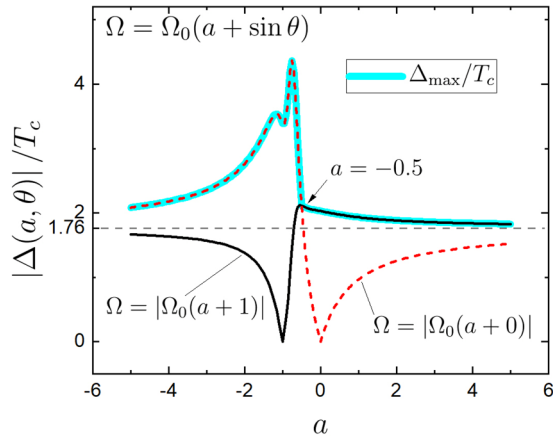
FIG. 6. $|\Delta_{\max}(0)|/T_c$ vs a for $\theta = 0$ (red dashed curve) and $\theta = \pi/2$ (black curve).

The absolute value of this ratio as a function of a is plotted for $\theta = 0$ and $\pi/2$ in Fig. 6.

After straightforward algebra we obtain for the anisotropy of penetration depth at T_c

$$\gamma_\lambda^2(T_c) = \frac{\langle \Omega^2 v_a^2 \rangle}{\langle \Omega^2 v_c^2 \rangle} = \frac{64 + 45\pi a + 80a^2}{120(4/15 + \pi a/4 + 2a^2/3)}. \quad (32)$$

This function is plotted in Fig. 7. The reason for the asymmetry of this plot relative to $a = 0$ is clear: For $a > 0$ the polar nodes no longer exist, and the phase becomes an anisotropic s. A similar situation takes place for $a \lesssim -1$, where the s part acquires a minus sign (or an extra phase shift of π). The most interesting part corresponds to the sharp drop in the curve in the interval $-1 \lesssim a \lesssim -0.5$, where the point polar nodes transform to line circular nodes on the altitude $\theta = -\arcsin a$.

Since on the Fermi sphere $\gamma_\lambda(0) = 1$, Fig. 7 gives an idea of how $\gamma_\lambda(T)$ may behave when the temperature varies from zero to T_c. We can see that for $a > -0.68$, where the curve of $\gamma_\lambda(t)$ (shown in red) crosses the line, $\gamma_\lambda = 1$; that is, in the anisotropic nodeless s phase $\gamma_\lambda(0) < \gamma_\lambda(T_c)$.
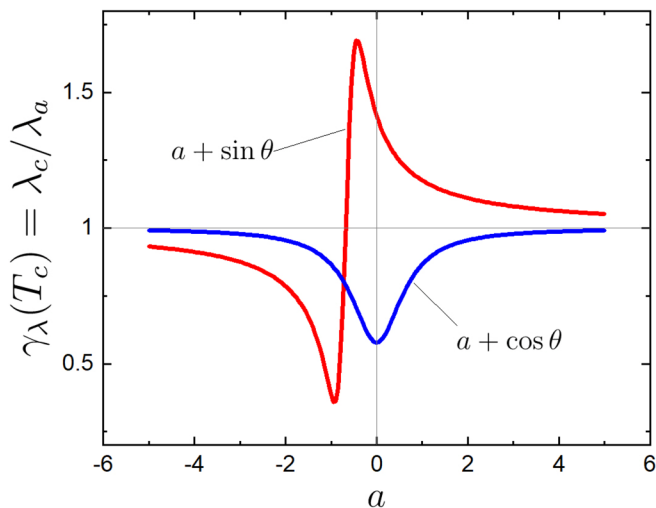

FIG. 7. $\gamma_\lambda^2(T_c)$ vs a for the order parameter $\Omega = \Omega_0(a + \sin\theta)$. $\gamma_\lambda^2(T_c) = 1$ at $a = -0.68$.
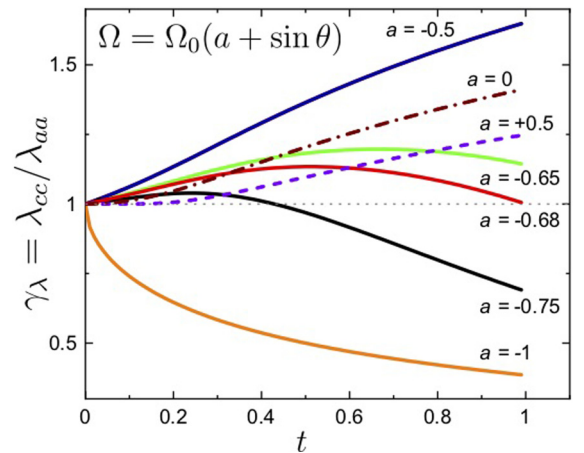

FIG. 8. γ_λ vs t for the order parameter $\Omega = \Omega_0(a + \sin\theta)$ for a set of a's indicated.

In a relatively narrow interval of values of the parameter a near $a \approx -0.7$, $(\gamma_\lambda - 1)$ changes quickly from positive to negative values, i.e., from increasing $\gamma_\lambda(t)$ to decreasing. The question then arises whether in this transformation domain $\gamma_\lambda(t)$ remains monotonic. Examples in Fig. 8 for $a = -0.75, -0.68$, and -0.65 show that this is not the case; $\gamma_\lambda(t)$ clearly has a well-pronounced maximum. Figure 8 demonstrates the evolution of the shape of $\gamma_\lambda(t)$ with changing weight a of the s-wave fraction in the order parameter $\Omega = \Omega_0(a + \sin\theta)$.

Thus, depending on the relative weight of two phases involved, we can have γ_λ increasing or decreasing on warming, the features commonly associated with multigap superconductivity.

F. $\Omega = \Omega_0(a\cos 2\varphi + \sin\theta)$

This mixture of the d-wave order parameter with line nodes at two meridians on the Fermi sphere and the polar point nodes differs from the previous example because polar nodes remain in the presence of the d wave, whereas line nodes do not survive due to the term $\sin\theta$. The treatment of this situation is similar to the cases considered, so we show only the results.

The anisotropy parameter $\gamma_\lambda(T_c)$ for this case is shown in Fig. 9. A sharp drop in the interval $-1 \lesssim a \lesssim 0.4$ resembles a similar drop for $\Omega = \Omega_0(a + \sin\theta)$, the mixture of the s wave and polar nodes. We expect a nonmonotonic $\gamma_\lambda(t)$ in the vicinity of $a \approx -0.4$, where $\gamma_\lambda^2(T_c) - 1$ changes sign. Indeed, we see this in Fig. 10. Hence, the maximum of $\gamma_\lambda(t)$ which we found for another mixed order parameter, $\Omega = \Omega_0(a + \sin\theta)$ (Fig. 8), was not accidental.

G. On the ratio of the experimental energy gap to T_c

The ratio $R = \Delta(0)/T_c$ is one of the fundamental superconducting parameters that can be measured experimentally. However, there is a great deal of confusion in experimental literature as to what one should expect within the weak-coupling BCS theory (which differs from the "strong-coupling" Eliashberg approach). Often this ratio, determined from spectroscopic measurements (scanning tunneling
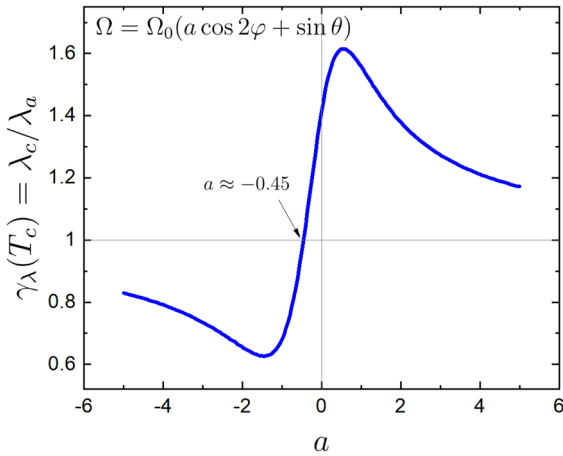
FIG. 9. $\gamma_\lambda(T_c)$ vs a for the order parameter $\Omega = \Omega_0(a \cos 2\varphi + \sin \theta)$.

microscopy, ARPES, optical reflectivity), is larger than that determined from thermodynamic experiments (the thermodynamic critical field H_c, the specific heat jump at T_c, the superfluid density). We have shown, however, that this ratio may exceed the BCS prediction of $R \approx 1.76$ within weak-coupling BCS models for anisotropic order parameters. Hence, the measured $R > 1.76$ might not serve as evidence of strong coupling.

The energy gap that enters the thermodynamics cannot exceed the isotropic s-wave BCS value of $\Delta(0)/T_c \approx 1.76$. Specifically, one can measure H_c, the specific heat jump at T_c, or the superfluid density to determine this gap. The condensation energy at $T = 0$

$$F(0) = \frac{H_c^2}{8\pi} = \frac{N(0)}{2}\langle \Delta^2(0) \rangle = \frac{N(0)}{2}\Psi^2(0), \quad (33)$$

which gives $\Psi(0) = H_c(0)/\sqrt{4\pi N(0)}$. According to Eq. (9) $\Psi(0)/T_c = 1.76 \exp(-\langle \Omega^2 \ln \Omega^2 \rangle/2)$. In all cases we have studied $0 < \langle \Omega^2 \ln \Omega^2 \rangle < 1$, so that $\Psi(0)/T_c$ does not exceed the weak-coupling value of 1.76. Hence, if we extract the gap from the data on H_c, the ratio R is expected to be less
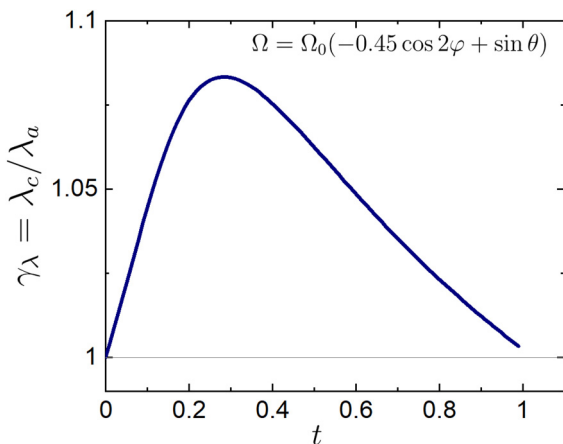

FIG. 10. γ_λ vs t for the order parameter $\Omega = \Omega_0(a \cos 2\varphi + \sin \theta)$ with $a = -0.45$.
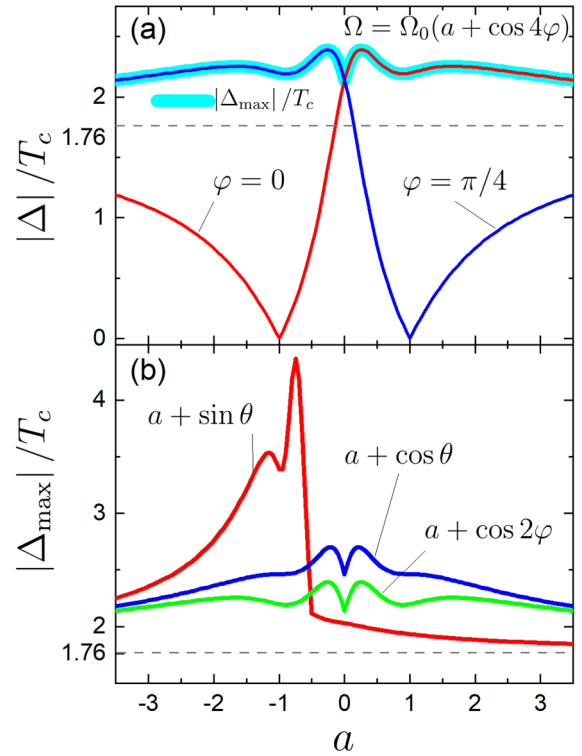

FIG. 11. (a) $\Delta(0)/T_c$ vs a, the weight parameter of admixture s phase, for order parameters $\Omega = \Omega_0(a + \cos 4\varphi)$ which describe ARPES data for KFe_2As_2 [21]. (b) $|\Delta_{max}(0)|/T_c$ vs a for order parameters indicated.

than 1.76. Also, measurements of the superfluid density [20] provide the magnitude of the order parameter $\Psi(T)$.

The specific heat jump is given in Eq. (27). In all cases we have considered $\langle \Omega^4 \rangle \geqslant 1$ (see Figs. 4 and 5), so that the jump is smaller than the isotropic value of 1.43.

The spectroscopic gaps (actually, the gaps in the quasiparticle spectrum) determined in ARPES, optical reflectivity, and tunneling experiments are a different story. Here, experiments give the maximum value of the superconducting gap:

$$\Delta_{max}(0) = |\Psi(0)\Omega_{max}(\mathbf{k})|. \quad (34)$$

The normalization $\langle \Omega^2 \rangle = 1$ implies that $\Omega_{max} \geqslant 1$, i.e., $\Delta_{max}(0) \geqslant \Psi(0)$. It is shown in Figs. 6 and 11 that, indeed, the ratio $\Delta_{max}(0)/T_c$ differs from the thermodynamic ratio $\Psi(0)/T_c$.

To conclude, the "thermodynamic" gap ratio is less than or equal to the isotropic weak-coupling BCS value of 1.76, whereas the maximum gap from spectroscopic experiments over T_c is greater than that. This difference led to often erroneous assignment of the larger than BCS values to the strong coupling. But the arguments we present here are developed, in fact, on the basis of the weak-coupling Eilenberger theory for anisotropic order parameters.

These arguments can be extended to multiband systems. Specifically, within the weak-coupling model of two-band superconductors, one gap will always be greater than the BCS value, and the other will always be smaller.

Thus, experimental ratios $\Delta_{max}(0)/T_c$ cannot be used to claim strong coupling without knowledge of the order param-

eter anisotropy. On the other hand, comparative analysis of thermodynamic and spectroscopic gaps may be used, if not to determine, definitely to restrict the possible order parameters for a particular material.

IV. DISCUSSION

The separable coupling model for one-band Fermi surfaces not only reproduces weak-coupling isotropic BCS thermodynamics but allows one to incorporate anisotropies of Fermi surfaces and of condensate order parameters. In particular, it provides a relatively straightforward procedure to obtain the temperature dependence of penetration depth and its anisotropy. As is the case in BCS, this procedure involves determination of the equilibrium order parameter $\Delta(T)$ by solving the self-consistency equation (the gap equation), a "labor-intensive" part in the anisotropic case. An alternative approach was given in Refs. [7–9], where an accurate analytic interpolation for $\Delta(T)$ was offered that could be used instead of solving the self-consistency equation.

We have verified this procedure for a number of different order parameters by comparing it with the numerical solutions of the self-consistency equation, and we found only small differences in the results that are insignificant as far as the accuracy of existing experimental data is concerned.

To separate possible effects of the order parameter anisotropy from those of Fermi surfaces, we considered only the Fermi sphere. We found that the anisotropy parameter of the penetration depth increases on warming for the order parameter with point nodes at the poles of the Fermi sphere, $\Omega = \sqrt{3/2}\sin\theta$. However, for the order parameter with a line node on the equator, $\Omega = \sqrt{3}\cos\theta$, $\gamma_\lambda(t)$ decreases. We have confirmed that for the d wave, $\Omega = \sqrt{2}\cos(2\varphi)$, $\gamma_\lambda(T) = 1$ at all temperatures, in agreement with previously calculated end point values $\gamma_\lambda(0) = \gamma_\lambda(T_c) = 1$ [6]. Thus, a common way to attribute the T dependence of $\gamma_\lambda(T)$ to different gaps at multiband Fermi surfaces is clearly questionable.

The possibility of a mixture of order parameters of different symmetries has been discussed for cuprates and other superconductors (see, e.g., [18,19,21]). Our analysis of the order parameter $\Omega = \Omega_0(a + \cos 2\varphi)$ showed that the anisotropy $\gamma_\lambda(T)$ depends on the relative phase of the constitutive order parameters (π for $a < 0$).

We have considered $\Omega = \Omega_0(a + \sin\theta)$, where a is the relative weight of the s-wave phase compared to the order parameter with polar nodes. First, we find that the ratio $\Delta_{\max}(0)/T_c$ may exceed considerably the standard weak-coupling value of 1.76 in a certain region of the parameter a (see Fig. 4). Second, it turned out that $\gamma_\lambda(T)$ may monotonically increase or decrease and even go through a maximum depending on the relative weight a of the two order parameters involved.

We have also tested the order parameter $\Omega = \Omega_0(a\cos 2\varphi + \sin\theta)$, i.e., a mixture of the d wave with the phase having polar nodes. Again, we see a maximum in $\gamma_\lambda(t)$ for the weight a near the value which corresponds to the end values $\gamma_\lambda(0) = \gamma_\lambda(T_c) \approx 1$ (Fig. 10). We speculate that if the experiment shows a nonmonotonic anisotropy of λ, the likely reason is a mixed order parameter. The last feature is intriguing in particular because we have an experimental

example of SrPt$_3$P in which $\gamma_\lambda(T)$ goes through a maximum [5].

As a by-product of our results we show in Fig. 11 the ratio $|\Delta(0)|/T_c$ vs the weight a of an admixture s phase for the order parameter $\Omega = \Omega_0(a + \cos 4\varphi)$ (the candidate for KFe$_2$As$_2$ [21]) for $\varphi = 0$ and $\pi/4$. It is worth noting that this ratio differs from the isotropic weak coupling BCS $\pi e^{-\gamma} = 1.76$; in fact, this ratio at certain admixtures of the s wave phase can be bigger or smaller than the BCS number. This, however, does not mean the coupling in these cases is strong or it is "weaker than weak"; rather, it is caused by the order parameter anisotropy. Note that the experimentally measured ratio is usually $|\Delta_{\max}(0)|/T_c = |\Psi(0)|\Omega_{\max}/T_c$.

APPENDIX: CLEAN CASE ORDER PARAMETER AT $T = 0$

Commonly, the effective coupling V is assumed to be factorizable [11], $V(\boldsymbol{v}, \boldsymbol{v}') = V_0\,\Omega(\boldsymbol{v})\,\Omega(\boldsymbol{v}')$. One then looks for the order parameter in the form $\Delta(\boldsymbol{r}, T; \boldsymbol{v}) = \Psi(\boldsymbol{r}, T)\,\Omega(\boldsymbol{v})$. The coupling constant V_0 is chosen to get the isotropic BCS result for $\Omega = 1$:

$$\frac{1}{N(0)V_0} = \ln\frac{2\omega_D}{\pi T_c e^{-\gamma}}, \tag{A1}$$

where ω_D is the energy scale of the "glue" excitations (of phonons in conventional materials) and $\gamma \approx 0.577$ is the Euler constant.

The self-consistency equation can be written in the form

$$\Psi(\boldsymbol{r}, T) = 2\pi T N(0)V_0 \sum_{\omega>0}^{\omega_D}\langle\Omega(\boldsymbol{v})f(\boldsymbol{v}, \boldsymbol{r}, \omega)\rangle. \tag{A2}$$

Since in the clean case $f = \Delta/\sqrt{\Delta^2 + \omega^2}$, we have, at $T = 0$,

$$\frac{1}{N(0)V_0} = 2\pi T \sum_{\omega>0}^{\omega_D}\left\langle\frac{\Omega^2}{\sqrt{\Delta^2 + \omega^2}}\right\rangle$$
$$= \left\langle\Omega^2\int_0^{\omega_D}\frac{d\omega}{\sqrt{\Delta^2 + \omega^2}}\right\rangle = \left\langle\Omega^2\ln\frac{2\omega_D}{|\Delta|}\right\rangle. \tag{A3}$$

Hence, as follows from (A3) and (A1) [9,13],

$$\frac{\Psi(0)}{T_c} = \frac{\pi}{e^\gamma}e^{-\langle\Omega^2\ln|\Omega|\rangle}. \tag{A4}$$

Clearly, for s-wave gaps, $\Omega = 1$ (at any Fermi surface) this gives $\Delta(0)/T_c = \pi e^{-\gamma} \approx 1.76$.

[1] J. Nagamatsu, N. Nakagawa, T. Muranaka, Y. Zenitani, and J. Akimitsu, Nature **410**, 63 (2001).

[2] J. D. Fletcher, A. Carrington, O. J. Taylor, S. M. Kazakov, and J. Karpinski, Phys. Rev. Lett. **95**, 097005 (2005).

[3] H. J. Choi, D. Roundy, H. Sun, M. L. Cohen, and S. G. Louie, Nature (London) **418**, 758 (2002).

[4] V. G. Kogan, Phys. Rev. B **66**, 020509(R) (2002).

[5] K. Cho, S. Teknowijoyo, S. Ghimire, E. H. Krenkel, M. A. Tanatar, N. D. Zhigadlo, V. G. Kogan, and R. Prozorov, arXiv:2101.06489.

[6] V. G. Kogan, R. Prozorov, and A. E. Koshelev, Phys. Rev. B **100**, 014518 (2019).

[7] F. Gross, B. S. Chandrasekhar, D. Einzel, K. Andres, P. J. Hirschfeld, H. R. Ott, J. Beuers, Z. Fisk, and J. L. Smith, Z. Phys. B **64**, 175 (1986).

[8] F. Gross-Alltag, B. S. Chandrasekhar, D. Einzel, P. J. Hirschfeld, and K. Andres, Z. Phys. B **82**, 243 (1991).

[9] D. Einzel, J. Low Temp. Phys **131**, 1 (2003).

[10] G. Eilenberger, Z. Phys. **214**, 195 (1968).

[11] D. Markowitz and L. P. Kadanoff, Phys. Rev. **131**, 563 (1963).

[12] V. L. Pokrovsky, Sov. Phys. JETP **13**, 447 (1961).

[13] V. G. Kogan and R. Prozorov, Phys. Rev. B **90**, 054516 (2014).

[14] L. P. Gor'kov and T. K. Melik-Barkhudarov, Sov. Phys. JETP **18**, 1031 (1964).

[15] V. Mishra, S. Graser, and P. J. Hirschfeld, Phys. Rev. B **84**, 014524 (2011).

[16] R. S. Gonnelli, D. Daghero, M. Tortello, G. A. Ummarino, Z. Bukowski, J. Karpinski, P. G. Reuvekamp, R. K. Kremer, G. Profeta, K. Suzuki, and K. Kuroki, Sci. Rep. **6**, 26394 (2016).

[17] Y. Zhang, Z. R. Ye, Q. Q. Ge, F. Chen, J. Jiang, M. Xu, B. P. Xie, and D. L. Feng, Nat. Phys. **8**, 371 (2012).

[18] L. A. Openov, JETP Lett. **66**, 661 (1997).

[19] G. Haran, J. Taylor, and A. D. S. Nagi, Phys. Rev. B **55**, 11778 (1997).

[20] R. Prozorov and V. G. Kogan, Rep. Prog. Phys. **74**, 124505 (2011).

[21] K. Okazaki *et al.*, Science **337**, 1314 (2012).